Journal of Theoretical Biology 430 (2017) 237–244

Contents lists available at ScienceDirect

Journal of Theoretical Biology

journal homepage: www.elsevier.com/locate/jtbi

Asymmetric disease dynamics in multihost interconnected networks

Shai Pilosof[a,1,*], Gili Greenbaum[b,c,1], Boris R. Krasnov[b], Yuval R. Zelnik[c]

[a] Department of Ecology and Evolution, University of Chicago, 1103 E 57 st, Chicago, 60637, USA
[b] Mitrani Department of Desert Ecology, Blaustein Institutes for Desert Research, Ben-Gurion University of the Negev, Sede Boqer Campus, 84990, Israel
[c] Department of Solar Energy and Environmental Physics, Blaustein Institutes for Desert Research, Ben-Gurion University of the Negev, Sede Boqer Campus, 84990, Israel

ARTICLE INFO

Article history:
Received 6 December 2016
Revised 18 July 2017
Accepted 20 July 2017
Available online 21 July 2017

Keywords:
Disease ecology
Epidemiology
Multilayer networks
Spreading dynamics

ABSTRACT

Epidemic spread in single-host systems strongly depends on the population's transmission network. However, little is known regarding the spread of epidemics across networks representing populations of multiple hosts. We explored cross-species transmission in a multilayer network where layers represent populations of two distinct hosts, and disease can spread across intralayer (within-host) and interlayer (between-host) edges. We developed an analytic framework for the SIR epidemic model to examine the effect of (i) source of infection and (ii) between-host asymmetry in infection probabilities, on disease risk. We measured risk as outbreak probability and outbreak size in a focal host, represented by one network layer. Numeric simulations were used to validate the analytic formulations. We found that outbreak probability is determined by a complex interaction between source of infection and between-host infection probabilities, whereas outbreak size is mainly affected by the non-focal host to focal host infection probability. Hence, inter-specific asymmetry in infection probabilities shapes disease dynamics in multihost networks. These results highlight the importance of considering multiple measures of disease risk and advance our understanding of disease spread in multihost systems. The study provides a flexible way to model disease dynamics in multiple hosts while considering contact heterogeneity within and between species. We strongly encourage empirical studies that include information on both cross-species infection rates and network structure of multiple hosts. Such studies are necessary to corroborate our theoretical results and to improve our understanding of multihost epidemiology.

1. Introduction

Understanding the transmission of disease among multiple hosts is a major endeavor of disease ecology because it provides insights into the possible impact of cross-species transmission on agriculture (e.g., transmission between wildlife and domestic animals), persistence of wild populations, and species conservation efforts (Böhm et al., 2009; Fenton and Pedersen, 2005; Langwig et al., 2012; Tompkins et al., 2003). For example, white-nose syndrome, induced by the fungus *Pseudogymnoascus destructans*, which invaded North America from Europe, is causing major declines in bat populations of several species (Blehert et al., 2009; Langwig et al., 2012). From a public health perspective, understanding cross-species transmission helps us understand the risk of zoonotic diseases (Daszak, 2000; Wolfe et al., 2007), with notable examples such as avian influenza and Ebola (Gire et al., 2014; Wang and Eaton, 2007).

Mathematical models of disease transmission across multiple hosts are typically mean-field models, which assume homogeneity in contacts within and between species (Craft and Caillaud, 2011; Fenton and Pedersen, 2005; Keesing et al., 2006). By contrast, network models consider heterogeneities in the contact structure (Bansal et al., 2007; Craft and Caillaud, 2011; Keeling and Eames, 2005) or other meaningful proxy for transmission (e.g., parasite sharing Pilosof et al., 2015; VanderWaal et al., 2013; 2014). This is important because heterogeneity in contacts can capture much of the variation in pathogen transmission (Craft and Caillaud, 2011; Pastor-Satorras et al., 2015). However, network models commonly represent a population of a single host species. Two main reasons can explain the paucity of multihost studies within a network analysis framework: (i) obtaining data on the contact networks within each species as well as data on interspecific contacts is extremely resource-intensive (Perkins et al., 2009); and, (ii) 'classic' network models are not adequate for modeling between-species contact heterogeneity because they contain a single network, representing

* Corresponding author.
E-mail addresses: shainova@gmail.com, pilosofs@uchicago.edu (S. Pilosof).
[1] Equal contribution.

http://dx.doi.org/10.1016/j.jtbi.2017.07.020
0022-5193/

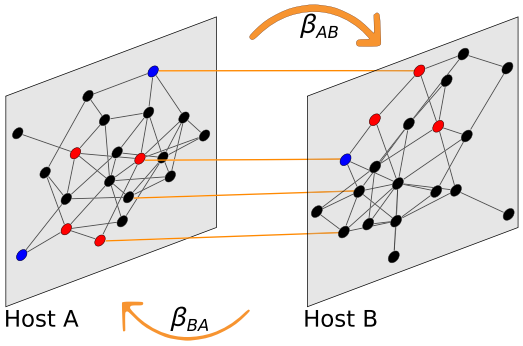

Fig. 1. A multilayer interconnected network between hosts A (left side) and B (right side). Intralayer edges (in black) represent contacts between individuals of the same host species. Interlayer edges (in orange) represent contacts between individuals of different host species. Infection probabilities between hosts A and B (β_{AB} and β_{BA}) may be asymmetric (represented by different width of orange arrows). Individuals can be susceptible (black nodes), infected (red nodes) or recovered (blue nodes). (For interpretation of the references to colour in this figure legend, the reader is referred to the web version of this article.)

a population of a single host species, disconnected from networks of other hosts. In this paper we address this second limitation.

One way to model disease spread across several hosts is with multilayer networks in which different layers can represent different host species. In particular, interconnected networks (as defined by Kivelä et al., 2014) are a useful representation because they contain two types of edges: *intralayer edges* connect individuals from the same population, while *interlayer edges* connect individuals from different populations (Fig. 1). Disease transmission in interconnected networks has been explored in the field of physics, and driven by human-related examples (reviewed in Boccaletti et al., 2014; Kivelä et al., 2014; Salehi et al., 2015). The main focus of these studies has been on modeling the conditions necessary for a disease to emerge (i.e., cross the $R_0 = 1$ threshold). Such conditions include the distributions of intralayer vs. interlayer edges in the network, which can create regimes whereby a disease spreads in one network but not in another (Dickison et al., 2012). For example, Saumell-Mendiola et al. (2012) have shown that when the correlation between the intralayer and interlayer degree distributions is strong, an outbreak may occur in the system even if it would not have occurred in any of the single layers alone. By contrast, in this paper we model disease transmission in interconnected multihost networks in a regime where the disease has already emerged (i.e., $R_0 > 1$) in order to study the outcomes of such epidemics.

We adopt an ecological point of view according to which an isolated network represents a population of a particular host species while an interconnected network represents a multihost system composed of populations of distinct host species (Fig. 1). For example, the transmission of bovine tuberculosis from badgers to cows may depend on the network structure of both species Böhm et al. (2009). This view is both realistic and necessary because (i) in multihost systems one host can alter the dynamics of pathogens in other hosts (Dobson, 2004; Fenton and Pedersen, 2005; Holt et al., 2003; Keesing et al., 2006) and (ii) these dynamics can be affected by the underlying network structure of each host Craft and Caillaud (2011).

In disease ecology, some multihost pathogen transmission models focus on the case in which a target species is infected by a source species (Fenton and Pedersen, 2005; Viana et al., 2014). In these models, little or no transmission from the target back to the source is assumed (Dobson, 2004; Viana et al., 2014). Other models deal with diseases that can be transmitted and maintained by more than one species (e.g., bovine tuberculosis or canine distemper virus). In this case, the dynamics of disease in the host of interest, which we term the *focal host*, may be affected by two factors inherent to multihost systems: (i) the source of infection — if the disease originates in the focal host itself or in a non-focal host; and (ii) the asymmetry in the rate of transmission between the two hosts. Both of these factors are of crucial importance for cross-species pathogen transmission (Craft et al., 2008; Dobson, 2004; Fenton and Pedersen, 2005). For example, recurrent infections from a non-focal host can cause endemic infection in a focal host even if the pathogen cannot establish in it (Fenton and Pedersen, 2005). Additionally, in zoonotic diseases the source of infection is the animal, rather than the human, causing strong asymmetry in infection dynamics; that is, probability of infection is higher from an animal species to humans than the other way around (Chapman et al., 2005; Wolfe et al., 2007).

Our goal is to understand how the interaction between these two factors affects disease dynamics in an interconnected network system. We quantify dynamics using two measures: (i) The probability of an outbreak, meaning the probability that a significant portion of the population is infected (see below); and (ii) the expected size of an outbreak (i.e., the proportion of the population infected), when an outbreak occurs. We develop an analytic framework to quantify outbreak size and probability in interconnected networks with asymmetric infection rates between the networks, in order to gain insights into multihost disease dynamics.

2. Modeling pathogen spread in interconnected networks

Following previous studies on interconnected networks (Dickison et al., 2012; Saumell-Mendiola et al., 2012; Wang et al., 2013), we use interconnected networks as depicted in Fig. 1. We refer to each of the single networks in an interconnected network as *layers* (Kivelä et al., 2014). Intralayer edges connect nodes within a layer while interlayer edges connect nodes from different layers. For simplicity, we considered the case of two interconnected populations (belonging to different hosts). We explore disease dynamics in layer A (L_A) of the interconnected network and thus consider L_A as our *focal host* species and layer B (L_B) as the *non-focal species* (Fig. 1). We define the mean number of interlayer edges connected to a node (or 'mean interlayer degree') in L_A as $e_A = \frac{E}{n_A}$, where E is the number of interlayer edges and n_A is the number of nodes in L_A. The mean interlayer degree in L_B is analogously defined as $e_B = \frac{E}{n_B}$.

We note that the networks we use are inherently different from models of disease spread in metapopulations, where the connection between populations is quantified via dispersal of individuals (Colizza and Vespignani, 2008) or from studies of interconnect transportation systems (Balcan et al., 2009). Instead, we focus on modeling epidemic spread in scenarios more relevant to multihost epidemics, where disease transmission occurs via contact or vector, and transmission is often asymmetrical. For example, the Ebola virus can be transmitted between groups of primates from different species (Walsh et al., 2007).

We study the spread of a pathogen in interconnected networks with an SIR model, in which each individual belongs to one of three compartments: susceptible (S), infected and thus infectious (I) or resistant and not infectious (R). It is advantageous to work with the SIR model because it is relevant for a vast range of diseases and because it is well established in the network epidemiology literature (Pastor-Satorras et al., 2015), providing us with a sound theoretical basis to build upon.

Following Begon et al. (2002), we denote the probability that a contact between an infectious and a susceptible individual leads to successful transmission of infection in a given time interval as β (this is the equivalent of ν from Begon et al., 2002). We hereafter refer to this parameter as *infection probability*. Because nodes in different layers belong to different species, the probability that a

susceptible individual will be infected by an infectious neighbor is determined by the species identity of both. Hence, β depends on the layers to which the two nodes belong (Dobson, 2004). We thus defined the infection matrix

$$\beta = \begin{bmatrix} \beta_{AA} & \beta_{AB} \\ \beta_{BA} & \beta_{BB} \end{bmatrix} \quad (1)$$

For example, β_{AB} is the probability that a node in L_A will be infected by a node from L_B. Individuals transition from an infected state to a recovered state after a given amount of time (the infectious period, τ), and the recovery rate is therefore $\gamma = \frac{1}{\tau}$ (sensu Keeling and Rohani, 2008).

We use the SIR model to examine two infection scenarios. In Scenario 1 the epidemic originates with an individual in L_A (the focal host) whereas in Scenario 2 it originates with an individual in L_B (the non-focal host). In both scenarios we track only the population of the focal host.

3. Analytic formulation of outbreak size and probability

The SIR spreading process on a network can be analytically studied by equating it with a bond percolation process (Keeling and Eames, 2005; Newman, 2002b). The bond percolation problem concerns diffusion through a discrete substrate to form clusters. In monolayer (non-interconnected) networks, the probability of a large outbreak and the expected size of such an outbreak in arbitrary random networks (random networks with any degree distribution) has been described by Newman (2002a). A percolation process on a network may be subcritical, in which case the diffusion is confined to a small number of nodes; Alternatively, it can be supercritical, in which case a *giant component* emerges and the diffusion process may cover a significant portion of the network. An outbreak can occur only when the system is in the supercritical phase; in epidemiological terms, this means that the disease crosses the $R_0 = 1$ threshold. Because we are interested in those settings where an epidemic may potentially have serious consequences for populations, we focus on scenarios in the supercritical phase.

The *transmissibility* of the pathogen via a given edge depends on both the infection probability and the recovery rate and is $T = 1 - (1 - \beta)^{\frac{1}{\gamma}}$ (Newman, 2002b). This property is a measure of the likelihood that the disease will be transmitted via a given edge if one of the nodes adjacent to it is infected. Transmissibility allows evaluating the size of an outbreak, if one occurs, by estimating the expected size of the giant component (i.e., the expected fraction of the network occupied by the giant component) in the percolation process on the network (Newman, 2002a; 2002b); that is, after keeping only a fraction of the original edges in the network along which the disease may be transmitted. For a large random network with an arbitrary degree distribution, both the size of the giant component, S, and the mean size of the non-giant components, s, can be calculated using percolation theory (see Appendix A). The size of the giant component corresponds to the size of an outbreak, since it is composed of exactly those nodes that will be infected if the epidemic originates in any node in the giant component. The probability that an epidemic starting in a random individual will result in an outbreak, P, is the same as the probability of belonging to the giant component, and thus in monolayer networks $P = S$ (Newman, 2002a; 2002b).

Applying percolation theory to interconnected networks is not straightforward, particularly when the infection probability is asymmetric ($\beta_{AB} \neq \beta_{BA}$). While the percolation process can describe the SIR dynamics in each of the layers separately (as for monolayer networks), the pathogen spreads across the interlayer edges with different probabilities in each direction. Therefore, there is no single transmissibility value for the interlayer edges, and the problem of finding the outbreak probability and size cannot be formulated as a simple percolation process. To provide approximation for outbreak size and probability in interconnected networks, we start by considering the percolation processes in each layer independently, as if they were disconnected. We then add the effect of the other layer for increasing the probability and size of outbreaks.

We assume (Assumption 1) that an outbreak in one layer will inevitably lead to an outbreak in the second layer. This is because the layers are sufficiently connected and outbreaks within layers are sufficiently large (when they occur), such that at least one interlayer edge will transmit the disease to the giant component in the other layer. Next, we consider the nature of the multihost setting. First, due to behavioral and life history differences between species, within-host contact rates are usually greater than between-host contact rates. Hence, there are less interlayer contacts than intralayer contacts per individual. Second, once two individuals come in contact, within-host infection probabilities are larger than between-host infection probabilities, for instance due to physiological competence between the host and the pathogen. This is a common assumption in virtually all multihost transmission models in disease ecology (Fenton and Pedersen, 2005; Holt et al., 2003; Poulin, 2007). It follows that interlayer transmission rates are lower than intralayer transmission rates. We combine these two assertions — low interlayer connectivity and low interlayer transmission rates — to a second assumption (Assumption 2), according to which each of the non-giant components formed by the bond percolation process is expected to transmit or receive the disease through *at most* one edge. That is, although it is permissible for non-giant components to have more than one interlayer edges connecting them, non-giant components cannot have more than one transmitting interlayer edge.

3.1. Probability of outbreak in interconnected networks

We wish to find the analytic solution to P_A — the probability of an outbreak in layer L_A. The probability of an outbreak in each of the layers if the interlayer edges are epidemiologically disconnected (i.e., $\beta_{AB} = 0$ and $\beta_{BA} = 0$) is the same as the size of the giant component in the percolation process in these layers; we denote these sizes as S_A and S_B. We further denote s_A and s_B as the mean number of nodes in the non-giant components in layers A and B, respectively, when the layers are disconnected. All these sizes — S_A, S_B, s_A, s_B — are functions of the intralayer infection probabilities (β_{AA} or β_{BB}), the recovery rates (γ_A or γ_B), and the relevant intralayer degree distribution (see Appendix A). Note that S_A and S_B are measured as a fraction of the network size, while s_A and s_B are measured in absolute number of nodes, rather than in fractions. When the layers are connected, the transmissibility of the pathogen from L_A to L_B via the interlayer edges is $T_{AB} = 1 - (1 - \beta_{AB})^{\frac{1}{\gamma_A}}$, where γ_A is the recovery rate of the host in L_A. This gives the probability that the pathogen spreads from an infected individual in L_A to a connected individual in L_B through a given interlayer edge. T_{BA} is analogously defined as $T_{BA} = 1 - (1 - \beta_{BA})^{\frac{1}{\gamma_B}}$.

In Scenario 1, an outbreak may occur as a result of intralayer transmissions within L_A if the node of origin belongs to the giant component. Alternatively, if the node of origin is not in the giant component, an epidemic may occur as a result of transmission to L_B causing an outbreak there which is then transmitted back to L_A. This will occur if (i) the non-giant component in which the disease originated is connected to L_B via an interlayer edge (with expected value $e_A s_A$); (ii) the interlayer edge transmits the disease to L_B (with probability T_{AB}); (iii) the node to which the pathogen is transmitted is in the giant component in L_B (with probability S_B).

Therefore, in Scenario 1

$$P_A = S_A + (1 - S_A)S_B e_A s_A T_{AB} \quad (2)$$

The first term in the equation refers to the case in which disease originates in the giant component whereas the second term refers to the concurrence of the three conditions mentioned, in the case where the disease originates in the non-giant component. We see that the probability of an outbreak depends only on the interlayer edge transmissibility in the direction $L_A \rightarrow L_B$. This is so because the infection in the other direction will occur if there is an outbreak in L_B, regardless of the transmissibility of the epidemic in the direction $L_B \rightarrow L_A$ (due to Assumption 1).

In scenario 2, the disease originates in L_B and the logic is analogous. An outbreak will occur in L_A if an outbreak occurs in L_B. Alternatively, if an outbreak does not occur in L_B, but (i) the non-giant component infected in L_B is connected with an interlayer edge (with expected value $e_B s_B$), (ii) this connecting edge transmits the epidemic (with probability T_{BA}), and (iii) the infection in L_A results in an outbreak (with probability S_A). The probability of an outbreak in this scenario is therefore:

$$P_A = S_B + (1 - S_B)S_A e_B s_B T_{BA}. \quad (3)$$

3.2. Outbreak size in interconnected networks

While in monolayer networks the size and probability of an outbreak are the same ($S = P$), this is not the case in interconnected networks, as we show below. In scenario 1, the size of an outbreak in L_A, which we denote as R^A_∞, is augmented by the possible infection of the non-giant components in the percolation process on that layer. Since we assume an outbreak occurs in L_A, an outbreak must occur in L_B as well. The giant-component in L_B may be connected via interlayer edges to non-giant component in L_A which may now become infected. The number of interlayer edges connected to the giant component in L_B is $S_B e_B n_B$, of which a fraction of $1 - S_A$ are connected to non-giant components in L_A. Each such infection in L_A increases the size of the outbreak by $\frac{s_A}{n_A}$ (due to Assumption 2). Therefore,

$$R^A_\infty = S_A + S_B(1 - S_A)s_A e_B \frac{n_B}{n_A} T_{BA} = S_A + S_B(1 - S_A)s_A e_A T_{BA}. \quad (4)$$

Notice that Eq. (4) is different from both Eqs. (2) and (3) in that only transmission in the direction $L_B \rightarrow L_A$ plays a role.

For scenario 2 the formulation is similar. Since we assume that an outbreak occurs in L_A, it is of no significance to the outbreak size where the epidemic originated, since an outbreak must occur in L_B. Therefore, L_B augments the outbreak in L_A in a similar manner as for Scenario 1, and Eq. (4) holds in this case as well. Therefore (and in contrast to the probability of an epidemic), only transmission rates in the direction $L_B \rightarrow L_A$ affect outbreak size, regardless of the source of the epidemic.

4. Numeric simulations of the spreading process

To test the analytic solutions, we compared them with numeric simulations. We used the Erdős–Rényi (ER) model as it is commonly considered as a 'null' network structure and because for the purpose of theoretical work, which aims to provide a general framework to generate predictions, the use of well-defined network models is advantageous (Newman, 2003). We find explicit solutions for the ER model (see Appendix A for derivation of S and s for ER networks), and compare them to simulation results. Natural animal or human networks do not necessarily fit into predefined network structures. Because our analytic framework is based on a derivation for random networks with any degree distribution (Newman, 2002b), it can be used to model a variety of different systems (see Appendix A). In this study we connected the layers uniformly at random (Dickison et al., 2012; Sahneh et al., 2013; Wang et al., 2013) such that on average, every node in layer A connects to one node in layer B ($e_A \approx e_B \approx 1$). It is important to remember, however, that in some cases nodes may be non-uniformly connected between layers. For example, males may be more territorial than females and thus have a stronger likelihood of interacting with individuals of other species, generating sex-biased connection patterns. Such non-random interlayer connectivity may affect the dynamics.

In multihost systems, infection probability is usually assumed to be lower (or equal, at most) between species than within-species (Fenton and Pedersen, 2005; Holt et al., 2003). We therefore considered $\beta_{AB}, \beta_{BA} \leq \beta_{AA} = \beta_{BB} = 0.03$. We chose to present results for $\beta_{AA} = \beta_{BB}$, but relaxing this assumption does not change the results qualitatively (see Appendix B). We tested for the effect of asymmetry in infection probability by varying β_{AB} and β_{BA} from 0 to 0.03 (including) in increments of 0.0005, resulting in $61 \times 61 = 3721$ (β_{AB}, β_{BA}) combinations. For each (β_{AB}, β_{BA}) combination, we randomly generated 100 interconnected networks, each of which was infected 1000 times, resulting in 100,000 simulations per combination. Each network had $n_A = n_B = 1000$ nodes and a mean degree of $< k >= 10$. However, we repeated those simulations for $n_A = n_B = 100$ and $n_A = n_B = 10,000$ and found that our results were qualitatively similar (see Appendix C). We set the infectious period $\tau_A = \tau_B = 6$. Each simulation was run until there were no more infected individuals.

Because disease dynamics are typically discussed in terms of R_0, rather than infection probabilities (β), we present the numerical results in terms of R_0 in Figs. 2 and 3, to facilitate the interpretation in a more general disease-ecology context. Within each of the layers, the simulation parameters translate to intralayer $R_0 = 1.8$: For layer L_A, $R_0 = \tau < k > \beta_{AA} = 6 \times 10 \times 0.03 = 1.8$, and similarly for layer L_B (as stated, we work at the $R_0 > 1$ regime within layers). Between layers, $R_0^{AB} = \tau\, e_A\, \beta_{AB}$, and R_0^{BA} is analogously defined. Since in our simulations interlayer infection probabilities range from 0 to 0.03, R_0^{AB} and R_0^{BA} values are in the range of 0 to 0.18. Qualitatively, because we maintain mean degree and infectious periods fixed, β's and R_0's behave similarly, and are interchangeable in the discussion that follows.

In each simulation, we calculated r_∞ — the final proportion of individuals in layer L_A (the focal host) who were infected at some point during the simulation. We then calculated two properties for each (β_{AB}, β_{BA}) combination:

1. The probability of an outbreak, $\mathcal{P}_A$, defined as the proportion of simulations (out of 100,000) in which the pathogen infected more than 10% of the population. While the selection of 10% is arbitrary, the exact value does not change the results. This is due to the strong bi-modality in the infection process, which is a consequence of the two types of components—giant and non-giant—rather than a continuous distribution of component sizes (Newman, 2002b). We compare $\mathcal{P}_A$ to P_A calculated using the analytic solution.
2. Outbreak size—the mean number of individuals infected in those simulations that have passed the 10% threshold, $\mathcal{R}^A_\infty$. We compare $\mathcal{R}^A_\infty$ to R^A_∞ calculated using the analytic solution.

Note that we use standard letters for notation of analytic parameters (e.g., P_A) and calligraphic letters for notation of parameters related to the simulations (e.g., $\mathcal{P}_A$).

The analytic framework is flexible enough to allow for any choice of parameters which satisfy our assumptions. For example, one could choose unequal infection probabilities or recovery rates for the two layers or other range of values for β_{AB}, β_{BA} (see example in Appendix B).

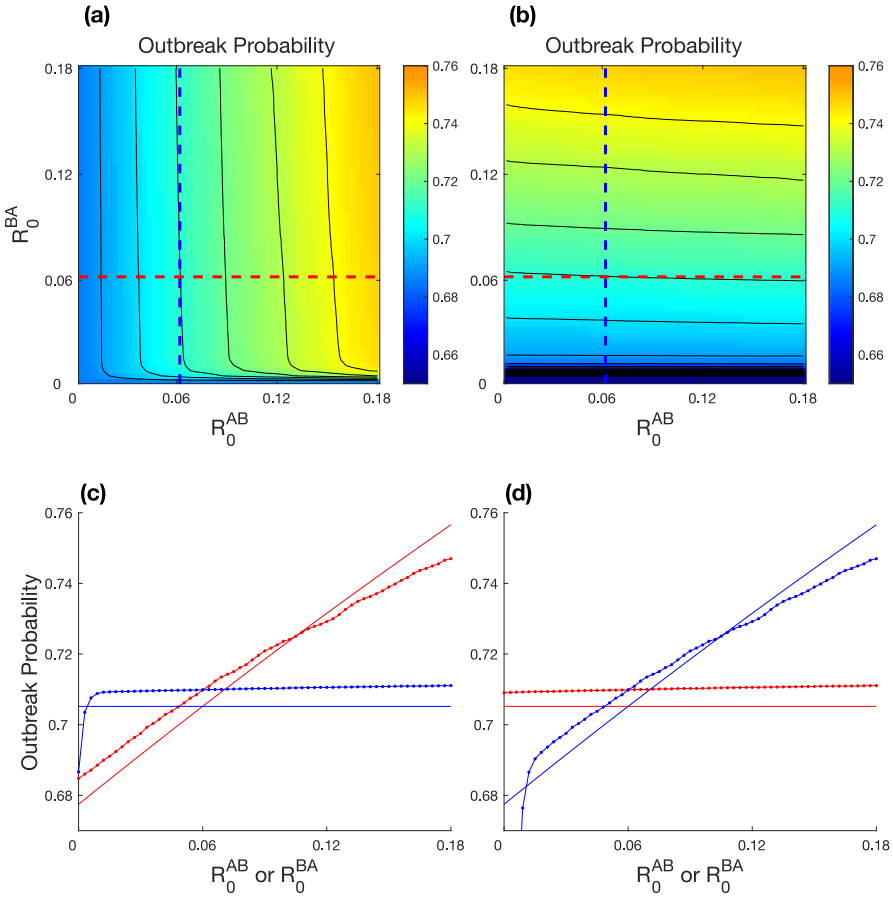

Fig. 2. Outbreak probability as a function of source of infection and interlayer R_0 values. Panels (a) and (b) depict the probability that a disease will infect at least 10% of the individuals in L_A (denoted as $\mathcal{P}_A$), when the disease originates in L_A (scenario 1) and L_B (scenario 2), respectively. In (c) and (d), colors represent cross-sections across $R_0^{BA} = 0.06$ (red) and $R_0^{AB} = 0.06$ (blue) in the parameter space of panels (a) and (b); solid lines are analytic solutions (denoted as P_A in the main text) and closed circles are simulation results ($\mathcal{P}_A$). Note that selecting a threshold other than 10% does not change the results. The analytic solutions are derived from Eqs. 2,3 and Appendix A. In (d), the Y-intercept of the numeric results for $R_0^{AB} = 0.06$ (blue) is at zero (not shown for clarity). Within each layer, $R_0 = 1.8$ (see text for details). (For interpretation of the references to colour in this figure legend, the reader is referred to the web version of this article.)

4.1. Effect on the probability of an outbreak

Eqs. (2) and (3) predict that the probability of an outbreak in the focal species, P_A, will strongly depend on the source of infection. This is so because these two equations differ in their parameters. Accordingly, we find in the simulations that when the disease originates in the focal host (L_A), β_{AB} determines $\mathcal{P}_A$ to a large extent (Fig. 2a), whereas when the disease originates in L_B, $\mathcal{P}_A$ is determined almost exclusively by β_{BA} (Fig. 2b). The reversal of the roles of β_{AB} and β_{BA} with different source of infections is illustrated by observing horizontal and vertical 'cross-sections' across the parameter space (Fig. 2c and d). It is evident from Fig. 2c that $\mathcal{P}_A$ increases approximately linearly with increasing β_{AB}, whereas it remains rather constant with changes in β_{BA}. The opposite pattern is evident in Fig. 2d, where $\mathcal{P}_A$ increases approximately linearly with an increase in β_{BA} but almost does not change with β_{AB}.

The emergence of this behavior is explained as follows. If an outbreak did not occur in the source layer (which can be either L_A or L_B), then there must be transmission from the source to the non-source layer (the terms on the right in Eqs. (2) and (3)) for an outbreak to still occur in L_A. This transmission is a function of the probability of infection from the source layer to the non-source layer. Once the infection traversed between layers, there are two options: (i) there is no outbreak in the non-source layer and the epidemic dies out (re-transmission back to the source layer is negligible due to assumption 2); (ii) there is an outbreak and transmission back to the source layer is almost certain. In this case the infection probability from the non-source to the source layer plays no role. Hence, both the source of infection and the asymmetry in interlayer transmission determine the behavior of $\mathcal{P}_A$.

4.2. Effect on outbreak size

In contrast to the marked qualitative effect of the source of infection on $\mathcal{P}_A$, it does not seem to have any major qualitative effect on the behavior of $\mathcal{R}_\infty^A$ (Fig. 3). The cross-sections show that $\mathcal{R}_\infty^A$ increases approximately linearly as β_{BA} increases but remains almost unaffected by β_{AB}, regardless of the source of infection. This is so because $\mathcal{R}_\infty^A$ is conditioned on an outbreak already occurring in L_A, and hence also in L_B. The additional increase in $\mathcal{R}_\infty^A$ (compared to the case where it is a monolayer network) is due to infections from the giant component in L_B to non-giant components in L_A (again, under our assumptions back-transmission from non-giant components is negligible). Therefore, the source of infection has no effect on $\mathcal{R}_\infty^A$. In addition, β_{AB} has no effect on $\mathcal{R}_\infty^A$ as evident from the line which is parallel to the x-axis in Fig. 3c and d (in red). This is in accordance with Eq. (4) which, as noted above, does not include transmission in the direction $L_A \rightarrow L_B$.

We note that in the scenario we simulated, we had equal intralayer transmission rates ($\beta_{AA} = \beta_{BB}$) and similar intralayer network structures, which resulted in quantitatively similar values for outbreak size and probability. However, this is not the general case

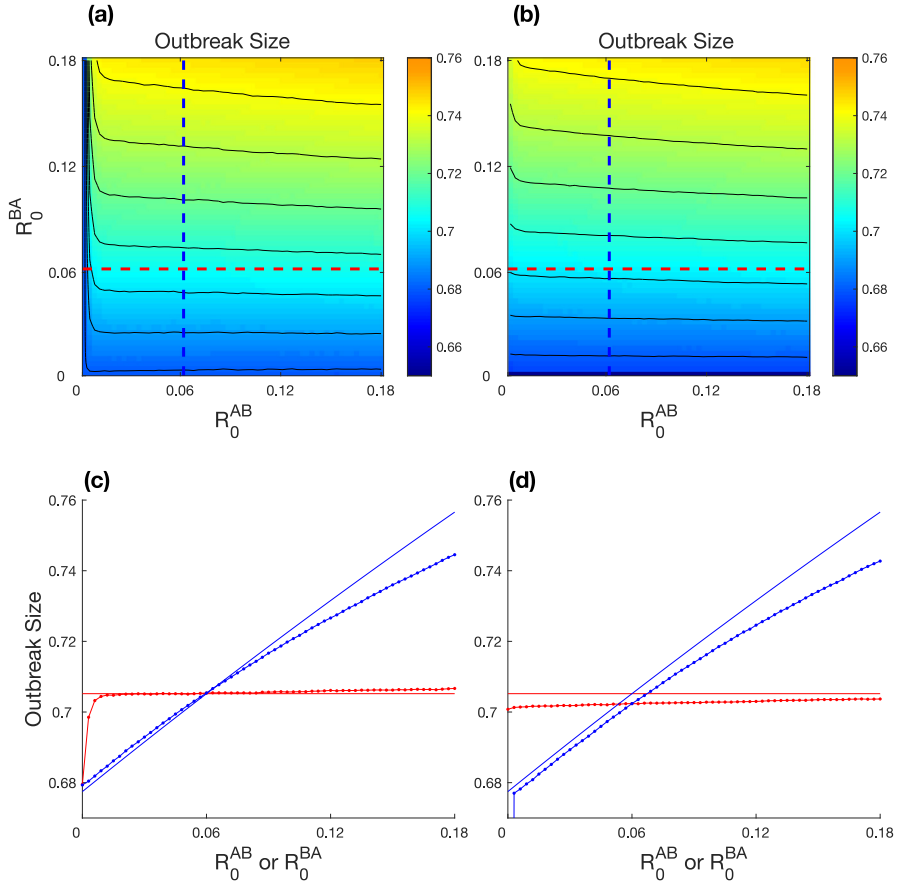

Fig. 3. Outbreak size as a function of source of infection and interlayer R_0 values. Panels (a) and (b) depict the mean number of individuals infected in those simulations that have passed the 10% threshold (denoted as $\mathcal{R}_\infty^A$), when the disease originates in L_A (scenario 1) and L_B (scenario 2), respectively. In (c) and (d), colors represent cross-sections across $R_0^{BA} = 0.06$ (red) and $R_0^{AB} = 0.06$ (blue) in the parameter space of panels (a) and (b); solid lines are analytic solutions (denoted as R_∞^A in the main text) and closed circles are simulation results ($\mathcal{R}_\infty^A$). The analytic solutions are derived from Eq. 4 and Appendix A. In (d), the Y-intercept of the numeric results for $R_0^{AB} = 0.06$ (blue) is at zero (not shown for clarity). Error bars are not included in panels (c) and (d) because the standard error of the mean was too small to show. Within each layer, $R_0 = 1.8$ (see text for details). (For interpretation of the references to colour in this figure legend, the reader is referred to the web version of this article.)

and even in this simple scenario outbreak size and probability behave qualitatively different (compare, for example, the trajectories of the red/blue lines in Figs. 2 and 3).

4.3. Limits of the analytic formulation

Overall, it is evident from Figs. 2 and 3 that the numeric simulations provide general support for the analytic solutions; however, there are several discrepancies which deserve attention and which also give us some insight into the infection process. Specifically, these discrepancies can help in identifying a parameter space in which the interdependent network can be studied through its layers.

For very low values of interlayer transmission rates, the analytic solutions significantly diverge from the numerical simulations. This is expected because when interlayer transmission is low, the system will behave more as a single network and less as an interconnected system. In such cases, even if an outbreak occurs in the layer where the disease originated, the second layer is likely to remain uninfected. This will violate Assumption 1 in regards to Eqs. (2)–(4). These equations describe the contribution of the two layers to outbreak probability and size, and are expected to overestimate the actual dynamics, as observed. We quantify and discuss the violations of Assumption 1 in the simulations more thoroughly in Appendix D.

We observe another discrepancy between the analytic and numeric solutions that increases as interlayer transmission rates increase (Figs. 2c,d and 3 c,d). Here, the analytic formulations predict a linear relation while the numeric simulations point to a slightly sub-linear one. One possible explanation for this observation concerns the expected contribution of the interlayer edges to transmission. The analytic formulations, under Assumption 2, consider the expected contribution of each transmitting interlayer edge as additive (to both probability and size of outbreak), since at most only one transmitting edge connects non-giant to giant components. However, when transmissibility is high enough, some interlayer edges which transmit the disease may connect to the same non-giant component, violating the assumption of additive contribution to outbreak size and probability. Therefore, at sufficiently high interlayer transmission rates, the analytic formulations will overestimate the actual dynamics. This process could be just one of several factors driving these deviations, particularly when the non-additive assumption is violated and complex feedbacks become likely. We quantify and discuss the violations of Assumption 2 in the simulations more thoroughly in Appendix D.

5. Discussion

In this work we bring together the theoretical aspects of the physics of infection processes on interconnected networks and of the disease ecology of multihost systems. We show how to model disease transmission in multi-host networks in ecological context, relaxing the simplifying assumptions of one-way or symmetric infection rates. The theory we present provides insights for multi-

host epidemics, as we show that asymmetry in interlayer infection probabilities and the source of infection jointly determine disease dynamics in multihost interconnected networks. Asymmetric infection rates between hosts have been documented in several disease systems. For example, Canine Distemper Virus in the Serengeti is spread among multiple carnivore families but with different probabilities (Craft et al., 2008). In New Zealand, bovine tuberculosis is transmitted among possums, feral pigs, deer and cattle but the role of each of these species in the overall dynamics of the disease is different due to differences in the persistence of the bacteria in each of the hosts and behavioral differences (Nugent, 2011). It may be valuable to investigate the joint effect of the multihost network structure and asymmetry in between-host infection rates on disease dynamics in such systems. Moreover, outbreak probability and size were affected differently by the source of infection, emphasizing the importance of considering different measures of disease risk, and a more detailed understanding of the mechanisms that underlie them.

We find that the dynamics in the focal host depends on whether the disease originated in this host itself or in the non-focal host. Many models of multihost pathogen transmission in disease ecology consider a target species infected by a reservoir source (disease originates in L_B and $\beta_{AB} \approx 0$; e.g., Dobson, 2004; Fenton and Pedersen, 2005). In the simulations, we assumed a constant maximum within-species infection probability and thus examine the continuum between emerging infectious diseases such as influenza ($\beta_{BA} \approx 0$) and true multihost diseases such as foot-and-mouth disease ($\beta_{AB} \approx \beta_{BA} \approx \beta_{AA} \approx \beta_{BB}$) (Fenton and Pedersen, 2005; Viana et al., 2014). On this continuum (and when the disease originates in the non-focal host), our results are consistent with previous studies as we show that the role of β_{AB} is minor in determining outbreak probability and size. In the case where between-host and within-host infection probabilities are equal (a true multihost pathogen; Fenton and Pedersen, 2005), dynamics will be determined only by the distribution of interlayer and intralayer edges. Dynamics in this class of network topology has been explored thoroughly in the context of network community structure (see Pastor-Satorras et al., 2015 for a review), but represent a particular case of the more general epidemic behavior we investigate here, which is often more relevant for disease ecology.

While one-way transmission is particularly relevant for zoonotic diseases, where identifying the source of infection is a major endeavor (Wolfe et al., 2007), the distinction between source and target hosts is blurred for many parasites which can switch between host species. For example, cowpox virus can infect both bank voles (*Clethrionomys glareolus*) and wood mice (*Apodemus sylvaticus*), with different infection probabilities (Begon et al., 1999) and humans and apes share several pathogens (Gómez et al., 2013). Moreover, infection probability is unique to a host-pathogen combination, resulting in among-host heterogeneity in infection probability to a given parasite (Streicker et al., 2013). Accordingly, our results show that considering between-host infection probabilities in both directions is crucial for disease outcomes. In addition, the qualitative difference in behavior of outbreak size and probability (in relation to the source of infection) highlights the need to include (asymmetric) two-way infections and consider the source of infection in multi-host epidemic models. For example, work on the shift of *Microbotryum violaceum*, the causal agent of anther-smut disease, between plant species of the genus *Silene* has shown that the transmission of the pathogen in both directions between the new and old plant hosts increases disease prevalence in both host plants (Antonovics et al., 2002), supporting our theoretical results.

Regardless of the host of origin, when the conditions and assumptions of our model are relevant, the non-focal host serves as an amplifier of the disease, in the sense that an increase in species richness increases disease risk (here measured as outbreak probability and size) (Keesing et al., 2006). This is clearly evident from Eqs. (2–4) which have two additive terms. However, the contribution of the non-focal host to epidemic size depends mainly on the transmissibility in the direction $L_B \rightarrow L_A$. Another way in which the non-focal host functions as a disease amplifier is that epidemiological cases in the focal host are not necessarily linked. This is because in networks, unlike in mean-field models, there are alternative routes for the infection to spread by carrying the disease to parts of the focal host network where it has not reached or would not have reached by infection within the focal host alone. This phenomenon becomes more likely with increasing between-species transmission.

Our study also has implications for the more general field of network science. Previous theoretical studies of epidemic spread in interconnected networks have focused on topological patterns that enable disease establishment (i.e., $R_0 > 1$), while assuming symmetry in interlayer infection probabilities (Boccaletti et al., 2014; Dickison et al., 2012; Salehi et al., 2015; Wang et al., 2013; Wang and Xiao, 2011). Only one study that we know of has addressed asymmetric rates of infection between two networks (Sahneh et al., 2013) but the authors investigated an analytic solution to the combination of infection probabilities that allows crossing the epidemic threshold ($R_0 > 1$). Hence, previous studies highlight the important role of interlayer feedbacks, where outcomes of dynamics cannot be extrapolated by analyzing each layer separately. By contrast, we identify a region of the parameter space within the supercritical regime ($R_0 > 1$), in which it is possible to understand overall system dynamics by integrating the dynamics evaluated for each layer separately. Additionally, our study advances the theory of diffusion in interconnected networks as it emphasizes that asymmetry in interlayer infection probabilities can change the expected diffusion dynamics due to a joint effect with the source of infection on epidemic size and probability.

One limitation of our simulation study is that the parameter values we have selected are somewhat arbitrary. The reason for that is the lack of empirical data of both within- and between-population contacts,together with information on infection probabilities. This is a reflection of the recently highlighted more general challenge of linking models to data in network epidemiology (Pellis et al., 2015). Such data is needed to corroborate if our two assumptions are indeed valid for natural systems, as well as to understand the parameter ranges that should be the focus of theoretical modeling. We thus emphasize the importance of data collection and the generation of multi-species data sets.

In conclusion, our findings contribute to a better understanding of disease dynamics in multihost systems on the one hand, and advance the theoretical understanding of epidemic spread in multilayer networks on the other. We hope that this and other studies which explore mechanistic models of disease spread in multihost networks will stimulate empirical studies, ultimately improving our predictive power of disease spread in multihost systems.

Code accessibility

We provide the complete code in the Figshare online repository (DOI:10.6084/m9.figshare.2058879).

Competing interests

We have no competing interests.

Funding

This research did not receive any specific grant from funding agencies in the public, commercial, or not-for-profit sectors.

Acknowledgements

SP was supported by a James S. McDonnell Foundation 21st Century Science Initiative – Postdoctoral Program in Complexity Science-Complex Systems Fellowship Award and by a Fulbright Fellowship from the U.S. Department of State. We thank Monika Böhm for helpful comments on previous drafts of this manuscript. This is publication no. 941 of the Mitrani Department of Desert Ecology.

Supplementary material

Supplementary material associated with this article can be found, in the online version, at 10.1016/j.jtbi.2017.07.020

References

Antonovics, J., Hood, M., Partain, J., 2002. The ecology and genetics of a host shift: microbotryum as a model system. Am. Nat. 160 (S4), S40–S53. doi:10.1086/342143.

Balcan, D., Colizza, V., Gonçalves, B., Hu, H., Ramasco, J.J., Vespignani, A., 2009. Multiscale mobility networks and the spatial spreading of infectious diseases. Proc. Natl. Acad. Sci. U. S. A. 106 (51), 21484–21489. doi:10.1073/pnas.0906910106.

Bansal, S., Grenfell, B.T., Meyers, L.A., 2007. When individual behaviour matters: homogeneous and network models in epidemiology. J. R. Soc. Interf. 4 (16), 879–891. doi:10.1098/rsif.2007.1100.

Begon, M., Bennett, M., Bowers, R.G., French, N.P., Hazel, S.M., Turner, J., 2002. A clarification of transmission terms in host-microparasite models: numbers, densities and areas. Epidemiol. Infect. 129, 147–153.

Begon, M., Hazel, S.M., Baxby, D., Bown, K., Cavanagh, R., Chantrey, J., Jones, T., Bennett, M., 1999. Transmission dynamics of a zoonotic pathogen within and between wildlife host species. Proc. R. Soc. London B 266, 1939–1945. doi:10.1098/rspb.1999.0870.

Blehert, D.S., Hicks, A.C., Behr, M., Meteyer, C.U., Berlowski-Zier, .B.M., Buckles, E.L., Coleman, J.T.H., Darling, S.R., Gargas, .A., Niver, R., Okoniewski, J.C., Rudd, R.J., Stone, W.B., 2009. Bat white-nose syndrome: an emerging fungal pathogen? Science 323 (5911), 227. doi:10.1126/science.1163874.

Boccaletti, S., Bianconi, G., Criado, R., del Genio, C.I., Gómez-Gardeñes, J., Romance, M., Sendiña Nadal, I., Wang, Z., Zanin, M., 2014. The structure and dynamics of multilayer networks. Phys. Rep. 544 (1), 1–122. doi:10.1016/j.physrep.2014.07.001.

Böhm, M., Hutchings, M.R., White, P.C.L., 2009. Contact networks in a wildlife-livestock host community: identifying high-risk individuals in the transmission of bovine TB among badgers and cattle. PLoS ONE 4 (4), e5016. doi:10.1371/journal.pone.0005016.

Chapman, C.A., Gillespie, T.R., Goldberg, T.L., 2005. Primates and the ecology of their infectious diseases: how will anthropogenic change affect host-parasite interactions? Evol. Anthropol. 14 (4), 134–144. doi:10.1002/evan.20068.

Colizza, V., Vespignani, A., 2008. Epidemic modeling in metapopulation systems with heterogeneous coupling pattern: theory and simulations. J. Theor. Biol. 251 (3), 450–467. doi:10.1016/j.jtbi.2007.11.028.

Craft, M.E., Caillaud, D., 2011. Network models: an underutilized tool in wildlife epidemiology? Interdiscip. Perspect. Infect. Dis. 676949. doi:10.1155/2011/676949.

Craft, M.E., Hawthorne, P.L., Packer, C., Dobson, A.P., 2008. Dynamics of a multihost pathogen in a carnivore community. J. Anim. Ecol. 77 (6), 1257–1264. doi:10.1111/j.1365-2656.2008.01410.x.

Daszak, P., 2000. Emerging infectious diseases of wildlife - threats to biodiversity and human health. Science 287 (5452), 443–449. doi:10.1126/science.287.5452.443.

Dickison, M., Havlin, S., Stanley, H.E., 2012. Epidemics on interconnected networks. Phys. Rev. E Stat. Nonlin. Soft Matter Phys. 85 (6 Pt 2), 066109. doi:10.1103/PhysRevE.85.066109.

Dobson, A.P., 2004. Population dynamics of pathogens with multiple host species. Am. Nat. 164 Suppl 5 (november), S64–78. doi:10.1086/424681.

Fenton, A., Pedersen, A.B., 2005. Community epidemiology framework for classifying disease threats. Emerg. Infect. Dis. 11 (12), 1815–1821. doi:10.3201/eid1112.050306.

Gire, S.K., Goba, A., Andersen, K.G., Sealfon, R.S.G., Park, D.J., Kanneh, L., Jalloh, S., Momoh, M., Fullah, M., Dudas, G., Wohl, S., Moses, L.M., Yozwiak, N.L., Winnicki, S., Matranga, C.B., Malboeuf, C.M., Qu, J., Gladden, A.D., Schaffner, S.F., Yang, X., Jiang, P.-P., Nekoui, M., Colubri, A., Coomber, M.R., Fonnie, M., Moigboi, A., Gbakie, M., Kamara, F.K., Tucker, V., Konuwa, E., Saffa, S., Sellu, J., Jalloh, A.A., Kovoma, A., Koninga, J., Mustapha, I., Kargbo, K., Foday, M., Yillah, M., Kanneh, F., Robert, W., Massally, J.L.B., Chapman, S.B., Bochicchio, J., Murphy, C., Nusbaum, C., Young, S., Birren, B.W., Grant, D.S., Scheiffelin, J.S., Lander, E.S., Happi, C., Gevao, S.M., Gnirke, A., Rambaut, A., Garry, R.F., Khan, S.H., Sabeti, P.C., 2014. Genomic surveillance elucidates ebola virus origin and transmission during the 2014 outbreak. Science 345 (6202), 1369–1372. doi:10.1126/science.1259657.

Gómez, J.M., Nunn, C.L., Verdú, M., 2013. Centrality in primate–parasite networks reveals the potential for the transmission of emerging infectious diseases to humans. Proc. Natl. Acad. Sci. U. S. A. 110 (19), 7738–7741. doi:10.1073/pnas.1220716110.

Holt, R.D., Dobson, A.P., Begon, M., Bowers, R.G., Schauber, E.M., 2003. Parasite establishment in host communities. Ecol. Lett. 6 (9), 837–842. doi:10.1046/j.1461-0248.2003.00501.x.

Keeling, M.J., Eames, K.T.D., 2005. Networks and epidemic models. J. R. Soc. Interf. 2 (4), 295–307. doi:10.1098/rsif.2005.0051.

Keeling, M.J., Rohani, P., 2008. Modeling Infectious Diseases in Humans and Animals. Princeton University Press, Princetone, New Jersey.

Keesing, F., Holt, R.D., Ostfeld, R.S., 2006. Effects of species diversity on disease risk. Ecol. Lett. 9 (4), 485–498. doi:10.1111/j.1461-0248.2006.00885.x.

Kivelä, M., Arenas, A., Barthelemy, M., Gleeson, J.P., Moreno, Y., Porter, M.A., 2014. Multilayer networks. J. Complex Netw. 2, 203–271. doi:10.1093/comnet/cnu016.

Langwig, K.E., Frick, W.F., Bried, J.T., Hicks, A.C., Kunz, T.H., Marm Kilpatrick, A., 2012. Sociality, density-dependence and microclimates determine the persistence of populations suffering from a novel fungal disease, white-nose syndrome. Ecol. Lett. 15 (9), 1050–1057. doi:10.1111/j.1461-0248.2012.01829.x.

Newman, M.E.J., 2002a. Random graphs as models of networks. In: Bornholdt, S., Schuster, H.G. (Eds.), Handbook of Graphs and Networks: From the Genome to the Internet. Wiley-VCH Verlag, pp. 34–68. doi:10.1002/3527602755.ch2.

Newman, M.E.J., 2002b. Spread of epidemic disease on networks. Phys. Rev. E Stat. Nonlin. Soft Matter Phys. 66 (1 Pt 2), 016128. doi:10.1103/PhysRevE.66.016128.

Newman, M.E.J., 2003. The structure and function of complex networks. SIAM Rev. 45 (2), 167–256. doi:10.1137/s003614450342480.

Nugent, G., 2011. Maintenance, spillover and spillback transmission of bovine tuberculosis in multi-host wildlife complexes: a new zealand case study. Vet. Microbiol. 151 (1–2), 34–42. doi:10.1016/j.vetmic.2011.02.023.

Pastor-Satorras, R., Castellano, C., Van Mieghem, P., Vespignani, A., 2015. Epidemic processes in complex networks. Rev. Mod. Phys. 87 (3), 925–979. doi:10.1103/RevModPhys.87.925.

Pellis, L., Ball, F., Bansal, S., Eames, K., House, T., Isham, V., Trapman, P., 2015. Eight challenges for network epidemic models. Epidemics 10, 58–62. doi:10.1016/j.epidem.2014.07.003.

Perkins, S.E., Cagnacci, F., Stradiotto, A., Arnoldi, D., Hudson, P.J., 2009. Comparison of social networks derived from ecological data: implications for inferring infectious disease dynamics. J. Anim. Ecol. 78 (5), 1015–1022. doi:10.1111/j.1365-2656.2009.01557.x.

Pilosof, S., Morand, S., Krasnov, B.R., Nunn, C.L., 2015. Potential parasite transmission in multi-host networks based on parasite sharing. PLoS ONE 10 (3), e0117909. doi:10.1371/journal.pone.0117909.

Poulin, R., 2007. Evolutionary Ecology of Parasites, second ed. Princeton University Press, Princetone, New Jersey.

Sahneh, F.D., Caterina, S., Chowdhury, F.N., 2013. Effect of coupling on the epidemic threshold in interconnected complex networks: A spectral analysis. In: 2013 American Control Conference doi:10.1109/acc.2013.6580178.

Salehi, M., Sharma, R., Marzolla, M., Magnani, M., Siyari, P., Montesi, D., 2015. Spreading processes in multilayer networks. IEEE Trans. Network Sci. Eng. 2 (2), 65–83. doi:10.1109/TNSE.2015.2425961.

Saumell-Mendiola, A., Serrano, M.A., Boguñá, M., 2012. Epidemic spreading on interconnected networks. Phys. Rev. E Stat. Nonlin. Soft Matter Phys. 86 (2 Pt 2), 026106. doi:10.1103/PhysRevE.86.026106.

Streicker, D.G., Fenton, A., Pedersen, A.B., 2013. Differential sources of host species heterogeneity influence the transmission and control of multihost parasites. Ecol. Lett. 16 (8), 975–984. doi:10.1111/ele.12122.

Tompkins, D.M., White, A.R., Boots, M., 2003. Ecological replacement of native red squirrels by invasive greys driven by disease. Ecol. Lett. 6 (3), 189–196. doi:10.1046/j.1461-0248.2003.00417.x.

VanderWaal, K.L., Atwill, E.R., Isbell, L.A., McCowan, B., 2013. Linking social and pathogen transmission networks using microbial genetics in giraffe (*giraffa camelopardalis*). J. Anim. Ecol. 83 (2). doi:10.1111/1365-2656.12137.

VanderWaal, K.L., Atwill, E.R., Isbell, L.A., McCowan, B., 2014. Quantifying microbe transmission networks for wild and domestic ungulates in kenya. Biol. Conserv. 169, 136–146. doi:10.1016/j.biocon.2013.11.008.

Viana, M., Mancy, R., Biek, R., Cleaveland, S., Cross, P.C., Lloyd-Smith, J.O., Haydon, D.T., 2014. Assembling evidence for identifying reservoirs of infection. Trends Ecol. Evol. 29 (5), 270–279. doi:10.1016/j.tree.2014.03.002.

Walsh, P.D., Breuer, T., Sanz, C., Morgan, D., Doran-Sheehy, D., 2007. Potential for ebola transmission between gorilla and chimpanzee social groups. Am. Nat. 169 (5), 684–689. doi:10.1086/513494.

Wang, H., Li, Q., D'Agostino, G., Havlin, S., Stanley, H.E., Van Mieghem, P., 2013. Effect of the interconnected network structure on the epidemic threshold. Phys. Rev. E Stat. Nonlin. Soft Matter Phys. 88 (2), 022801. doi:10.1103/PhysRevE.88.022801.

Wang, L.-F., Eaton, B.T., 2007. Bats, Civets and the Emergence of SARS. In: Childs, J.E., Mackenzie, J.S., Richt, J.A. (Eds.), Wildlife and Emerging Zoonotic Diseases: The Biology, Circumstances and Consequences of Cross-Species Transmission. Springer Berlin Heidelberg, pp. 325–344.

Wang, Y., Xiao, G., 2011. Effects of interconnections on epidemics in network of networks. In: Wireless Communications, Networking and Mobile Computing (WiCOM), 2011 7th International Conference on, pp. 1–4. doi:10.1109/wicom.2011.6040146.

Wolfe, N.D., Dunavan, C.P., Diamond, J., 2007. Origins of major human infectious diseases. Nature 447 (7142), 279–283. doi:10.1038/nature05775.